NASA TECHNICAL MEMORANDUM

NASA TM X-71503

NASA TM X-71503

(NASA-TM-X-71503) JET NOISE FROM CO-AXIAL NOZZLES OVER A WIDE RANGE OF GEOMETRIC AND FLOW PARAMETERS (NASA) 30 p HC $3.50 CSCL 20A

N74-17405

Unclas
G3/23 29460

JET NOISE FROM CO-AXIAL NOZZLES OVER A WIDE RANGE OF GEOMETRIC AND FLOW PARAMETERS

W. Olsen and R. Friedman
Lewis Research Center
Cleveland, Ohio 44135

TECHNICAL PAPER proposed for presentation at
Twelfth Aerospace Sciences Meeting sponsored by the
American Institute of Aeronautics and Astronautics
Washington, D.C., January 30 - February 1, 1974

JET NOISE FROM COAXIAL NOZZLES OVER A WIDE RANGE OF GEOMETRIC AND FLOW PARAMETERS

W. Olsen and R. Friedman
Lewis Research Center
National Aeronautics and Space Administration
Cleveland, Ohio

Abstract

Free field pure jet noise data were taken for a large range of coaxial nozzle configurations. The core nozzles were circular (1 to 4 in. diam.) and plug types. The fan to core area ratio varied from 0.7 to 43.5, while the velocity ratio typically varied from 0 to 1. For most cases the two nozzles were coplanar but large axial extensions of either nozzle were also tested. Correlation of the data resulted in a simple procedure for estimating ambient temperature subsonic coaxial jet noise spectra over a wide range of geometric and flow parameters.

Introduction

E-7873

In many of today's civil aircraft, takeoff noise is dominated by jet noise, which is a major annoyance to the communities near airports. The earliest jet engines were turbojets which had a single high velocity jet exhaust. Then a small fan was added so that there were two exhaust streams issuing from coaxial nozzles. The fans in these turbofan type engines have gradually increased in size. For the same thrust, turbofans propel more air at a lower jet velocity than the turbojet engine. The lower jet velocity results in reduced jet noise.

Subsonic coaxial nozzle jet noise has been investigated by a number of recent investigators.[1-3] The data cover a limited range of nozzle size and shape, velocity, and angle. A series of ambient temperature coaxial jet noise experiments have been conducted at the NASA Lewis Research Center. The main purpose of these experiments was to acquire more complete data for coaxial nozzles over a wide range of size, shape, and velocities. The large variation in physical size and shape should prove useful in evaluating jet noise theories and in generating more accurate coaxial jet noise predictions for engine trade-off studies.

The core nozzles tested were circular and plug types, with the core nozzle diameters of 1 to 4 inches. The fan to core nozzle area ratio varied from 0.7 to 43.5. A very high bypass ratio turbofan engine, for example, might have an area ratio of about 4. The subsonic core velocities ranged from 600 to 1000 ft/sec. The fan nozzle to core velocity ratio was generally varied in steps from 0 to 1. For the plug nozzle tests most of the data were taken with a cone shaped plug (no flow separation), but in a few cases a flat ended plug was used for comparison to show the effect of flow separation. Most of the data were taken with coplanar fan and core nozzles. Tests were also run with a very large core nozzle extension. In addition, the fan nozzle lip was extended beyond the core nozzle to as much as 6 fan nozzle diameters so that the fan and core jets would be partially to fully mixed before exiting to the environment. The jet noise associated with a three exhaust-stream coaxial nozzle was also measured. Finally, tests were made to describe the noise radiation pattern of engine fan and turbine noise individually passing through a coaxial nozzle (simulated by a dominant internal noise placed upstream of the nozzle).

The test apparatus provided free field jet noise data unaffected by valve noise. Far field axisymmetric noise was measured with eleven half-inch condenser microphones around the half circle from the nozzle inlet to the exhaust. The data consisted of sound pressure level spectra and their spectral and spatial integrations. A small sample of the total data taken in this program are presented herein. Comparisons are also made with the data taken by other investigators. The spectral data are correlated in a number of summary plots which can be used as part of a subsonic ambient temperature coaxial jet noise prediction scheme.

Apparatus and Procedure

Flow System and Valve Noise Quieting

Two separate but similar flow lines were used to supply air independently to the two nozzles that make up the coaxial nozzles investigated herein (Fig. 1). Each flow line was attached to the laboratory pressurized air supply. Each flow line consisted of the following elements (proceeding downstream): a flow control valve, a valve noise quieting section, inlet pipe, and finally the test nozzle. The inner or core nozzle had a long straight length of 8-inch pipe for its inlet. The outer or fan nozzle used 16-inch pipe, which then split into two 12-inch branches and finally came together in a large plenum, with screens located upstream of the fan nozzle. Velocity profile measurements indicated uniform velocity profiles across and circumferentially around the core and fan nozzle exits. The velocities in the plumbing (pipes, elbows, muffler, and plenums) were kept below 150 ft/sec so that they would not produce significant internal noise. The turbulence intensity at the nozzle exit planes was less than 1 percent. The valve noise quieting section in each line consisted of a perforated plate orifice followed downstream by a large no-line-of-sight muffler. None of the nozzle jet noise data reported herein were affected by internal valve or flow noise, either through the nozzle exit or by direct radiation. To prevent direct valve noise radiation, Fiberglas and lead vinyl insulation was wrapped around all the plumbing upstream of the nozzle. The fan nozzle inlet plenum was then wrapped externally with Fiberglas to reduce jet noise reflections. The nozzle stagnation temperature varied according to the season from about 40° to 80° F.

Acoustic Instrumentation and Data Analysis

The noise data were measured outdoors with a vertical semicircular microphone array of 15-foot radius centered on the nozzle exit (Fig. 1(b)).

Eleven microphones were used that were more closely spaced (10^o to 15^o intervals) near the nozzle jet than in the upstream quadrant (15^o to 20^o intervals). The angle $\theta_I = 0^o$ is directed upstream. This vertical circular array of half-inch condenser microphones (with windscreens) was located above 6-inch thick acoustic foam on the ground. This microphone and foam arrangement resulted in free field noise data in the far field for frequencies above 400 Hz. The microphones were calibrated before and after each day's run with a piston calibrator (a 124 dB tone at 250 Hz).

The noise data were analyzed directly by an automated one-third octave band spectrum analyzer, which was periodically recalibrated, and also checked with a pink noise generator. The analyzer determined sound pressure level spectra, SPL, referenced to 0.0002 microbar (2×10^{-5} N/m^2). A small fraction of the data required corrections. Background noise affected the low noise level data below 400 Hz; the data were corrected to remove this contribution. Generally three samples of data were taken so that occasional transient background noises could be eliminated by a voting and averaging scheme in the data processing program. A small correction (about 2 dB at 20 kHz) was also made, according to SAE ARP866,(4) for atmospheric losses so that the data reported are lossless. These SPL spectra were then used to compute the overall sound pressure level, OASPL, at each microphone position. Occasionally the peak SPL occurred too close to the highest frequency recorded (20 kHz), causing the computed OASPL to be too low. These SPL spectra were extrapolated and the OASPL was thereby corrected (less than 2 dB). Lip noise, which is a non-jet noise (generally affecting a few 1/3 octave bands near or above 20 kHz), was also not included in the OASPL. The sound power level spectrum, PWL, and total sound power level, PWL_T, were computed by a spatial integration of the SPL spectra. The spatial integration used the "bread slice" elements for this axisymmetric noise, as described in Ref. 5.

From the microphone calibrations, periodic checks of the data system, and redundant data it was estimated that the data were repeatable from day to day to about 1 dB and a third octave band. Most of the directly compared data were taken on the same day, and these data were repeatable to about 1/2 dB. In Ref. 6, some of the single stream jet noise spectral data obtained from this facility were compared to scaled up data taken by Lush in an anechoic chamber(7); the agreement was within the day to day repeatability.

The data reported herein are considered to be accurate, lossless, far and free field pure jet noise.

Test Nozzles

Figure 2 contains sketches of the two-stream coaxial nozzles tested and part of the nozzle inlet geometry. Because the nozzle flange was far enough upstream and the nozzle inlets were not excessively large, there was no significant jet noise reflection or shielding affecting the noise radiation pattern at angles greater than 30^o. Figure 2(a) schematically shows the coplanar nozzle configuration that was used for most of the tests. The range of core diameter, d_C, was from 1 to 4 inches, and the range of fan nozzle diameter was from 3.35 to 8.7 inches. The nozzles have a gradual inlet and short thin lip. The velocity profiles, measured at the nozzle exits, were uniform. Therefore, the jet velocities reported herein were accurately computed by isentropic theory from the nozzle stagnation pressure and temperature.

Figure 2(b) shows the 2.8 inch diameter plug insert which is supported by thin airfoil shaped struts in the low velocity core plenum. Two plug ends were tested: a cone end with no flow separation, and a flat ended plug.

Figures 2(c) and (d) show the core and fan nozzle extension configurations. The core nozzle extension shown in Fig. 2(c) has a gradual but large area reduction at the end, which resulted in a uniform core velocity profile at the exit, with no flow separation of the external fan flow. A short and a very long core nozzle extension were tested. The fan nozzle extensions in figure 2(d) allowed comparisons of the effect of partial and complete internal jet mixing on coaxial jet noise. Complete internal mixing is essentially attained within six fan diameters. In addition, a nozzle was attached to the fan extension pipe to determine its effect on the noise produced.

Test Procedure

Far field noise and flow data were taken for a number of nozzle configurations at various nozzle jet velocities. Generally the core velocity was set, for a given nozzle configuration, and the fan velocity was varied so that the fan to core velocity ratio was varied in about seven steps from 0 to 1. In cases where the outer nozzle was large, the higher velocity ratios could not be reached. The core velocity generally ranged from 600 to about 1000 ft/sec, with most of the data taken near 1000 ft/sec.

Results and Discussion

The data in this report, and in Refs. 1 and 2, indicate that the fan flow essentially modifies the basic core jet noise levels and spectra. Accordingly, the coaxial jet noise results herein are discussed in three major sections. The first section deals with correlations of the jet noise spectral data for the baseline single stream nozzle (i.e., core jet alone). The second section considers the effect of the fan flow (i.e., the effect of fan to core velocity and area ratios) upon the jet noise for a coaxial nozzle using coplanar circular nozzles. The third section deals with geometrical variations from the coplanar circular nozzle geometry of the previous sections. There is also a discussion of the noise radiation pattern of simulated fan and turbine internal noise.

Single Stream Nozzle Jet Noise

A description of jet noise for a single stream nozzle requires a description of its noise level and its spectra. The noise level for ambient temperature subsonic single stream nozzles was described in Ref. 6. However, jet noise spectra have not been adequately described. A correlation of jet noise spectral data is required.

The ambient temperature subsonic jet noise spectral data are described herein by a series of spectral templates, one for each angle, whose shape is essentially unaffected by nozzle size and only slightly affected by the jet velocity. The location of the peak noise on each template is defined by its level, SPL_p, and frequency, f_p. For an ambient temperature jet, the location of the peak noise (SPL_p, f_p) is a function of jet velocity, nozzle size, and angle. The peak noise level, SPL_p, is determined by two relationships. One empirically relates the difference, OASPL-SPL_p, to the angle. The other relationship is for the total intensity, OASPL, which was defined in Ref. 6 as a function of nozzle size, jet velocity, and angle. Once the peak noise is located in noise level and frequency space (SPL_p, f_p), then the spectral template for that angle defines the rest of the noise spectrum.

Figure 3 shows the spectral shape curves (templates) for jet noise at a number of angles, for $1\frac{5}{8}$- , 4-, and 6-inch diameter nozzles at high and low subsonic velocities.[6,8] The spectral data are plotted in a manner that describes the jet noise spectra relative to the peak noise (SPL_p, f_p), which is determined as described above. A gradual change in the spectral shape occurs with angle. The change in shape is rapid near the jet axis, where refraction is important. The spectral shape is also broader near the jet axis at the low jet velocities than for the high velocities. The template curves were constructed as follows. Each spectral data set for a given nozzle velocity and angle, was translated (without rotation) as a unit in order to get the best agreement between the data sets at each angle. This translation was required for two reasons. One is caused by the variation of f_p with velocity and size. The other is due to the fact that the spectral shape was observed to translate by as a whole by as much as 1 dB and a third octave band in long term repeatability experiments. After the data sets are collapsed together one average smooth curve was drawn through the data points for each angle and velocity as shown on Fig. 3. The difference between the total intensity and peak noise level (OASPL-SPL_p) is calculated from these curves and noted on Fig. 3; this difference is used later.

These spectral templates were then used to locate the peak noise frequency, f_p, of other single stream nozzle jet noise data, which covered a subsonic velocity range of 600 to 1000 ft/sec and a nozzle diameter range of from 1 to 6 inches.[6,8] The location of the peak noise (SPL_p, f_p) can be quite accurately determined because the applicable template is translated until the best overall fit is obtained for the 20 to 25 data points of a spectral set. The resulting experimental values of f_p, referenced to the f_p at $\theta_I = 90^o$, are plotted on Fig. 4 as a function of angle, θ_I. These data show that there is no f_p variation with angle in the upstream quadrant ($\theta_I \leq 90^o$), but for $\theta_I > 90^o$ there is a rapid change in f_p with angle. There appears to be a small effect of velocity but only near the jet axis.

All that remains to be done is to relate f_p at $\theta_I = 90^\circ$ to the jet velocity, V_C, and the nozzle size, d_C. This was accomplished by using the following equation

$$f_p\left(\theta_I = 90^\circ\right) = 1.0\,\frac{V_C}{d_C} \tag{1}$$

With the baseline single stream (or core jet alone) noise correlated the next task is to consider the modifications of the core noise caused by the fan flow.

Coplanar Coaxial Nozzle Jet Noise Data

In this section the modification of the single jet noise caused by the addition of the fan flow to the core flow is considered. It will be shown that the noise level of a coaxial nozzle is essentially a modification of the core-nozzle-alone peak noise level and frequency. The spectral template that described the core-alone jet noise spectra is unchanged by the fan flow. The template just translates as a function of the coaxial nozzle parameters.

Noise Level. The influence of the fan flow upon the noise level and noise radiation pattern shape is considered in this section. The data taken in this study and in Ref. 1 both show that the shape of the noise radiation pattern is independent of the fan flow. In other words the pattern shape is unaffected by changes in the coaxial nozzle parameters (i.e., the fan to core area ratio, $AR = A_F/A_C$, and velocity ratio, $VR = V_F/V_C$). The pattern shape is the same as for the core nozzle alone. Only the noise level changes as a function of the coaxial nozzle parameters, VR and AR. Based on these results the following equation was written to describe the noise level and radiation pattern for the coaxial nozzle.

$$\text{OASPL} = 10\log_{10}\Bigg[\underbrace{\frac{K}{R^2}\frac{\rho_o^2}{c_o^4}A_C V_C^8 \overbrace{\left(1 - \frac{0.62\,V_C}{c_o}\cos\theta_J\right)^{-3}}^{\text{Shape of noise radiation pattern}}}_{\text{Core jet alone noise level}}\;\underbrace{\Gamma\left(AR, VR\right)}_{\text{Effect of fan flow}}\Bigg] + C \tag{2}$$

The coefficient, K, which is determined from single stream jet noise data at $\theta_J = 90^\circ$, is equal to 3.2×10^{-6}. The core-jet-alone noise level is described by the first group of terms while the effect of the fan flow on the noise level is described by Γ, which is a function of only the coaxial nozzle parameters, VR and AR. The noise radiation pattern shape is described in Eq. (2) by the term with the -3 exponent, which was derived for single stream circular nozzles by Goldstein and Howes.[9] Reference 6 pointed out that this term described the shape of the single stream subsonic jet noise radiation patterns for circular, slot, plug, and mixer nozzles, and also circular hot jets, except near the jet axis where refraction is important. The theory of Ref. 9 neglects refraction, shear noise relative to self-noise, and the effect of nonisotropic turbulence.[10]

Figures 5(a) through (c) contain plots of coaxial nozzle jet noise radiation patterns over a very large range of velocity and area ratios and core velocities. The plots show that the noise radiation pattern shape is not affected by the fan flow parameters, VR and AR. Only the noise level is affected by VR and AR through the $\Gamma\langle VR,AR\rangle$ term of Eq. (2), which is discussed later. The noise radiation pattern shape term of Eq. (2) can be fitted to the data quite well. Figures 5(a) through (c) show that only the core velocity is required to describe the pattern shape, provided $VR \leq 1$. A small correction was made, by means of Eq. (2), to the data on Fig. 5 and subsequent figures so that they are all normalized to a common environmental temperature of 77° F.

Spectra. Figure 6 contains the noise spectra for coplanar circular coaxial nozzles over a range of velocity ratios, for several combinations of core nozzle size, area ratio, and angle, θ_I. In Fig. 6(a) the core diameter is 3 inches, the area ratio is 2.1, and the data were taken at a 90° angle from the inlet. The single stream spectral template curve for 90° is drawn through the data for each VR to give the best overall fit. The peak noise location from the template is located with an X for each VR. The peak noise locus curve looks like a part of a loop. Figure 6(b) contains the same type of plot, at an angle of 90°, for a 3-inch core nozzle with an area ratio of 3.9. The spectra for a 2.08-inch core nozzle and an area ratio of 9.3 are plotted on Fig. 6(c). The 90° template again fits these data for each VR quite well. Figure 6(c) contains data at an angle of $\theta_I = 135°$ for the 3-inch nozzle considered in Fig. 6(b). The 135° spectral template was fitted through these data with equal success. The resulting peak noise locus curve appears to be essentially the same shape as the one obtained at 90° in Fig. 6(b).

Because the templates fit the spectral data so well, only the locus curves are required to define the spectra completely for a given set of coaxial nozzle parameters. Figure 7 contains a group of these locus curves. Figures 7(a) and (b) show the effect of area ratio for 3- and 2.08-inch core nozzles, respectively. The locus curves are shaped like part of a loop, with the minimum noise level, SPL_p, occurring between VR = 0.4 and 0.5, and the minimum frequency, f_p, occurring between VR = 0.5 and 0.6. As the area ratio increases the loops get larger. Figure 7(c) shows that the core velocity does not affect the shape of the locus curve. Figure 7(d) shows that the locus curve shape is not affected by the angle, θ_I. The same locus curve shape would also result if the power spectra were plotted for each VR. The locus curves were translated in Figs. 7(c) and (d) because the core noise was not the same.

These results show that the shape of the peak noise locus curve only depends upon AR and VR. The location of the locus curve in SPL - frequency space, however, depends on the SPL_p and f_p coordinates for the core nozzle alone.

One of the main points of Figs. 6 and 7 was that the coaxial jet noise spectrum was described by the spectral template for that angle for the entire test range of VR, AR, and core diameter and velocity. The spectral shape template simply translates through noise level-frequency space as a function of those parameters. But for exceptionally large area ratios this simple model tends to fail near a velocity ratio of 0.4. Figure 8 contains the noise spectra for a coaxial nozzle with an area ratio of 43.5. The 90° single peak spectral template fits all velocity ratio cases except 0.4, where a double peak occurs. The same type of spectrum occurred with a coaxial nozzle having an area ratio of 27, but the single peak spectrum did fit the AR = 16.4 data. This result was not caused by extraneous noise sources such as valve noise.

Correlation of Coaxial Jet Noise

It was shown that the fan flow (i.e., VR and AR) did not affect the spectral shape. Changes in VR and AR merely translated the core-nozzle-alone spectral template along a peak noise locus curve. The shape of the locus curve was only a function of AR and VR, while the location of the locus curve in SPL - frequency space depended on the core alone parameters. Therefore, the objective of this section is to determine the peak noise location (SPL_p, f_p) as a function of the fan flow parameters (AR,VR) and the core parameters.

Noise Level. In this section the effect of the fan flow on the noise level is correlated. According to Eq. (2), the function Γ, or $10 \log_{10} \Gamma$ in decibel units, must be evaluated. This log term would be equal to the difference between the coaxial nozzle noise level and the core alone noise level (in dB), for a given θ_I and fixed core conditions. It was shown that Γ is only a function of area and velocity ratio (i.e., $\Gamma\langle AR,VR\rangle$). Figure 9 contains a plot of the variation of $10 \log_{10} \Gamma$ with area ratio and velocity ratio, for a number of core nozzles. The solid curves for $\Gamma\langle AR,VR\rangle$ are described by Eq. (3), which is a variation of the semiempirical model suggested by Williams.[1]

$$\Gamma\langle AR,VR\rangle = (1 - VR)^{1.1\sqrt{AR}} + 1.2 \frac{VR^{0.01}}{(1 + AR)^3} (1 + AR\, VR^2)^4 \qquad (3)$$

The exponent, $1.1\sqrt{AR}$, is not permitted to exceed 6, and $VR^{0.01}$ was used because it has a value of unity except very near VR = 0. The data generally scatter, within a 2 dB band, about these curves, the greatest scatter occurring near VR = 0.6.

Since Γ is not a function of angle, it can be evaluated from many sources of data. Most of the data used in Fig. 9 represent Γ determined from the change in OASPL at 90°. The same result was also obtained using the change in total sound power. The change in sound power data reported in Ref. 2 and the change in OASPL at 120°, measured by Williams,(1) are also plotted on Fig. 9. The results from the literature closely agree with the results obtained in this study.

Results from the SAE model are plotted on this figure as dashed curves. The SAE coaxial jet noise prediction(11) assumes each jet (the fan and core) generates noise independently. This means the noise cannot be less than the core alone, which is obviously erroneous for $VR \leq 0.6$, based on Fig. 9. However, this prediction is accurate for $VR \geq 0.8$, which is where most present day turbofan engines operate.

To summarize, the peak noise level, SPL_p, is determined from Eq. (3) for $\Gamma\langle AR,VR\rangle$, Eq. (2) for the OASPL, and Fig. 3 for $(OASPL-SPL_p)$.

<u>Spectra</u>. When the peak noise level, SPL_p, has been determined all that remains to be done in order to completely define coplanar coaxial jet noise is to determine the frequency of the peak noise, f_p, as a function of VR and AR. With SPL_p and f_p determined, the spectral templates can then be positioned to describe the whole of the coaxial jet noise spectral surface, $SPL\langle f,\theta_I\rangle$. From the peak noise locus curves of Fig. 7, and other similar data, the variation in f_p with VR and AR can be determined. Figure 10 contains a plot of the peak noise frequency ratio as a function of VR and AR. The peak noise frequency ratio, $F_{pR}\langle AR,VR\rangle$, is defined as the f_p, measured at VR and AR, divided by the f_p of the core jet alone (at $VR = 0$). The f_p for the core alone is determined from Eq. (1) and Fig. 4. Average smooth curves are drawn through the data for each velocity ratio, VR. The $VR = 0.4$ curve is not drawn for $AR > 16$ because of the two-peaked spectra that develop at $VR = 0.4$ somewhere between an AR of 16.4 and 27. The data scatter generally within a one-third octave wide band from these curves. While the data shown are for $\theta_I = 90^\circ$ and a core velocity of about 985 ft/sec, the same overall results are obtained at other angles and core velocities.

To summarize, the peak noise frequency, f_p, of a coaxial nozzle is determined by the following relationship.

$$f_p = \underbrace{F_{pr}\langle\theta_I\rangle\left(\frac{1.0\ V_C}{d_C}\right)}_{\text{Core jet alone}} \underbrace{F_{pR}\langle AR,VR\rangle}_{\text{Effect of fan flow}} \qquad (4)$$

where $F_{pr}\langle\theta_I\rangle$ is determined from Fig. 4 and $F_{pR}\langle VR,AR\rangle$ is determined from Fig. 10.

At $VR = 1$ the coaxial nozzle might be expected to act as a single nozzle whose diameter is that of the fan nozzle. This would mean that at

VR = 1 the peak noise frequency ratio would equal the fan diameter divided by the core diameter.

$$F_{pR}\langle AR, VR = 1\rangle = (1 + AR)^{-1/2} \qquad (5)$$

This is plotted on Fig. 10 as a dashed curve. But, the VR = 1 data lie one or two one-third octave bands above this curve (i.e., data at higher frequency). Perhaps this is due to the presence of the extra turbulence caused by the boundary layer flow over the core nozzle surfaces.

The data contained herein, and hence the correlation, are limited to ambient temperature jets. It is likely that a hot core jet will at least affect the core alone jet noise near the jet axis.

Effect of Geometrical Changes from Two Coplanar Circular Nozzles

Plug Core Nozzle. The previous results were obtained with circular core nozzles; this section deals with plug core nozzles. At VR = 0 the spectral shape and noise radiation pattern for a well designed practical plug nozzle can be expected to be nearly the same as an equivalent area circular nozzle; but the noise level would be slightly lower by 1 to 2 dB.[6] In Fig. 11(a) the spectra for several core geometries (plug and circular) are compared at the same core velocity, for velocity ratios of 0, 0.5, and 1.0. The core areas and area ratios are slightly different so the results were scaled slightly (according to Eq. (2) and Figs. 9 and 10) to bring all results to a common core area and area ratio. The three circular nozzle cases collapse together. As expected, while the plug nozzle spectra shape is essentially the same as the circular core nozzles, the plug nozzle proves to be slightly quieter at all velocity ratios.

More extensive plug-coaxial nozzle data were taken than shown in Fig. 11(a). These data agree with the circular-coaxial nozzle data plotted on the correlation curves for the effect of the fan flow (Figs. 9 and 10). The noise radiation pattern shapes for the plug coaxial nozzle were also essentially the same as for the circular nozzle. Therefore, the only significant difference between the plug and circular core coaxial nozzles was that the plug nozzle was 1 to 2 dB quieter than the equivalent area circular nozzle.

In Ref. 6 it was demonstrated that a poorly designed plug, that suffers from considerable flow separation, generates significantly more noise than one with no flow separation. A blunt ended plug of extreme flow separation was compared to the cone plug discussed above that had no flow separation. These plugs were compared as part of the same plug-coaxial nozzle (Fig. 2(b)). As shown in Fig. 11(b), the blunt ended plug was about 4 to 8 dB noisier than the case with the cone plug when there was no fan flow (VR = 0). At VR = 0.5 the flow separation noise greatly exceeds the jet noise at high frequency. At VR = 1, the noise levels come together because the fan jet noise dominates over the flow separation noise. The blunt ended plug is an extreme academic example of flow separation, but the results point out the importance of avoiding flow separation in a suppressor nozzle, such as the coaxial nozzle, operating at conditions near maximum suppression (e.g., VR = 0.5).

Extended Core Nozzle. The velocity in the fan exhaust will decay as it flows downstream. If the core nozzle is extended a considerable distance downstream of the fan nozzle, then a jet velocity ratio of unity might become a local velocity ratio of about 0.5 at the core exit plane. A greatly extended core nozzle might therefore have its minimum coaxial jet noise occurring at VR = 1. The core extension test nozzles had an area contraction at the exit as shown by Fig. 2(c). This resulted in a low turbulence uniform velocity profile at the core exit. The noise from a long core nozzle extension (56 annulus heights long) was compared to a short core nozzle extension (8.5 annulus heights long). The outer nozzle size would have to be changed in order to directly compare to a coplanar nozzle, but Fig. 11(a) shows that the short core nozzle extension coaxial nozzle produced the same noise as an equivalent size coplanar circular coaxial nozzle. Therefore the long extension is effectively compared to a coplanar nozzle. Figure 12 contains a comparison of the power spectra for the long and short core nozzle extensions for three velocity ratios (VR = 0, 0.5, 1.0). The spectra are the same for VR = 0 and 0.5. But when VR = 1 the long core extension is somewhat quieter at low frequencies. The velocity profile was measured at the core exit plane for the short core extension. The fan nozzle exhaust velocity profile there is rounded but the peak velocity is the same as the fan jet velocity (i.e., $V_E/V_F = 1$). In the case of the long core extension, the fan exhaust (peak velocity) decayed to half of fan jet velocity, $V_E/V_F = 0.5$, by the time it reached the core exit plane.

In conclusion, a small noise reduction can be achieved at VR = 1 by a core nozzle extension, but only if it is extremely long.

Extended fan nozzle. In many engine designs the fan nozzle is extended beyond the core nozzle exit plane. This permits some mixing of the hot core and cold fan flows, which can theoretically increase the thrust. The extended fan nozzle geometry tested herein is shown in Fig. 2(d). In this case the fan nozzle extension was a constant diameter pipe. The fan extensions tested ranged from 2 to 6 fan nozzle diameters long (e.g., $L_F/d_F = 2,4,6$). Complete internal mixing occurred (i.e., the velocity profile is essentially unaffected by additional length) for the 6 diameter long case[1] and partial mixing occurred with the shorter lengths.

The extended fan nozzle cases are compared to the coplanar nozzle case ($L_F/d_F = 0$) at the same core nozzle exit plane velocities (V_F, V_C). Figure 13(a) shows the change in noise as the velocity ratio ($VR = V_C/V_F$) was varied for each of the extension cases ($L_F/d_F = 2,4,6$). The change in noise is the change from the coplanar nozzle case at VR = 0 (for coplanar nozzles VR = 0 is acoustically equivalent to running without the fan nozzle, AR = 0). This comparison is for an area ratio of 3.9, a core velocity of 740 ft/sec and a core nozzle diameter of 3 inches. The data show that there is a small decrease (less than 2 dB) in the noise level for velocity ratios greater than 0.8 when the fan nozzle is extended. The spectral data (Fig. 13(b)) and noise radiation pattern are also essentially unchanged. Williams[1] noted essentially the same result in a similar experiment with smaller nozzles. At the low velocity ratios there was a general increase in the noise level at all frequencies (see Fig. 13(a) and (b)). For the $L_F/d_F = 2$ and 4 cases there was an additional intense low frequency broadband howling noise. The noise radiation pattern for these low velocity ratio cases peaked at about $\theta_I = 130^o$ while the coplanar and high velocity cases peaked near 160^o. The former result is characteristic of an internal noise source, while the latter is characteristic of an external noise source. The table contained in Fig. 13(a) indicates the extended fan nozzle exhaust plane peak (centerline) velocity, V_E, for each case, compared to the core velocity (V_C = 740 ft/sec). For the large velocity ratio cases there was very little decay of the centerline velocity (i.e., $V_E/V_C \simeq 1$). This fact coupled with the fact that the noise radiation pattern is characteristic of an external noise source, indicate that the major part of the jet noise is generated by the external exhaust jet for the high velocity ratio cases. At low velocity ratios most of the noise is being generated within the extended fan nozzle.

Similar tests were performed with a nozzle of small contraction (upstream area/nozzle exit area = 1.2) attached to the extended fan nozzle exit. The core nozzle exit plane velocities (V_C,V_F) were the same as for the no exit nozzle cases described above. This exit nozzle caused V_E/V_C to exceed 1 except at very low velocity ratios. Therefore the external jet was even more clearly the dominant noise source except at very low VR, where there was still an intense howling noise.

These extended fan nozzle results point out that the majority of the jet noise occurs wherever the velocity decay is largest. In these ambient temperature experiments, the peak (centerline) velocity did not decay much internally at the high velocity ratios; therefore, the external jet was the dominant jet noise source. If the core jet were hot there may be more internal decay; therefore, the results may be different.

Three-stream nozzle. If each stage of a two-fan stage turbofan engine were exhausted separately, then the resulting engine would have three exhaust streams. One such arrangement was tested and the results are shown in Fig. 14. In this configuration the fan (middle nozzle) to core area ratio was 2.1, the outer nozzle to fan nozzle area ratio was 0.78, and the core diameter was 3 inches. The outer nozzle to fan nozzle velocity ratio, V_o/V_F, varied from 0.8 to 0.7 as the fan to core velocity, VR = V_F/V_C, was changed from 1.0 to 0.5. For comparison, the outer nozzle was blocked and the resulting two stream nozzle was run at the same velocity ratios, VR. Even though the total flow for the three stream nozzle was much larger it was slightly quieter than the two stream nozzle at the same VR and core conditions.

Noise Radiation Pattern of Internal Noise

This section discusses tests performed in order to describe the noise radiation pattern of engine fan and turbine noise passing through a coaxial nozzle. These noise sources were simulated by a dominant internal noise placed upstream of each nozzle.

A dominant internal noise of high frequency was first placed in the core nozzle plenum and the fan flow was varied from VR = 0 to 1, for a fixed core velocity. The internal noise was generated by a half-inch orifice that exhausted far upstream into the core nozzle plenum. At a frequency of 10 kHz the internal noise was at least 6 dB more than the jet noise at all angles, for velocity ratios between 0 and 1. The pressure ratio across the noise orifice was held constant so that the internal noise level would be nearly constant. The sound power level, PWL, at 10 kHz did in fact remain constant with the internal noise in the core. Figure 15(a) shows how this constant power internal core noise distributes spatially (i.e., noise radiation pattern) at a frequency of 10 kHz for velocity ratios of 0, 0.5, and 1 at core velocities of 600 and 860 ft/sec. The noise radiation pattern for internal core noise passing through a nozzle appears to peak near $\theta_I = 110^o$, and is fairly independent of the fan or core flow. Refraction caused by the fan flow reduced the noise near the jet axis only about 4 dB.

The same experiment was repeated with the internal noise placed instead in the fan nozzle plenum. In this case the PWL at 10 kHz varied some with VR, so the noise levels had to be adjusted. Figure 15(b) shows that almost the same radiation pattern as Fig. 15(a) resulted, but with the peak noise moved downstream to 120^o. In these experiments the wave length of the internal noise is much less than the nozzle diameter; this is also the case for turbofan engines. The ambient temperature results in Figs. 15(a) and (b) are typical of engine turbine and fan noise radiation patterns in that they also peak near 120^o.[12] These data should prove useful in evaluating engine noise data, which is a complex mixture of noise sources.

Summary of Results

Free field pure jet noise data were taken for a large range of coaxial nozzle configurations. The core nozzles were circular (1 to 4 in. diam.) and plug types. The fan-to-core area ratio varied from 0.7 to 43.5, while the velocity ratio typically varied from 0 to 1. For most cases the two nozzles were coplanar, but large axial extensions of either nozzle were also tested. The data and correlations are limited to ambient temperature jets.

The important results and correlations are described below.

1. The fan flow from a coaxial nozzle essentially modifies the core nozzle alone jet noise. The noise level, OASPL, for the coaxial nozzle is equal to the multiple of two terms. The first term describes the core

nozzle alone noise level and radiation pattern. The second term, Γ, which is the only term dependent on the fan flow, affects only the noise level. The minimum noise level for a given nozzle and core velocity occurs at a fan to core velocity ratio of 0.4 to 0.5. The coaxial nozzle noise level data are well correlated by the semiempirical relations presented herein. These data agree well with the previous coaxial jet noise data reported by T. Williams and G. Bielak.

2. The SPL spectral shape at a given angle did not significantly change with core nozzle size, or with the velocity and area ratios. In other words, if the location of the peak noise (both level, SPL_p, and frequency, f_p) is known, then the spectral shape (template) for that angle could be used to construct the complete spectrum. These spectral templates are given in the text. The peak noise level, SPL_p, is determined from the OASPL. The peak noise frequency, f_p, for a coaxial nozzle is equal to the multiple of three terms. The first two terms describe the peak noise frequency for the core jet noise alone. The last term is the ratio of the coaxial noise to the core alone noise, and is only a function of the velocity and area ratios. The minimum f_p occurs at a velocity ratio of 0.5 to 0.6.

3. The preceding results are for coplanar circular coaxial nozzles; the following results are for different nozzle geometries.

(a) The only significant difference between plug and circular coaxial nozzles of the same area is that the noise level of the plug nozzle is 1 to 2 dB quieter. Any flow separation off the plug can generate considerable noise except at the high velocity ratios.

(b) Extending the core nozzle well beyond the fan nozzle had only a small effect on the noise, compared to the coplanar nozzles result.

(c) Fan nozzle extension configurations are slightly quieter than the coplanar configuration at high velocity ratios, but an intense low frequency broadband howling noise is generated within this fan nozzle extension at the low velocity ratios.

Nomenclature

A_C core nozzle area at exhaust plane, ft^2

A_F fan nozzle area at exhaust plane, ft^2

A_o third (outer) nozzle area, ft^2

AR fan to core area ratio, A_F/A_C

C constant to account for reference conditions and unit conversion factors

c_o	speed of sound in environment, ft/sec
d_C	core nozzle diameter, ft
d_F	fan nozzle diameter, ft
$F_{pR}\langle VR, AR \rangle$	peak noise frequency ratio of coaxial nozzle; f_p for coaxial nozzle at VR and AR, divided by f_p for core alone ($V_R = 0$)
$F_{pr}\langle \theta_I \rangle$	peak noise frequency ratio of the core; f_p at θ_I divided by f_p at $\theta_I = 90^o$
f	third octave band center frequency, Hz
f_p	frequency of the peak noise intensity, Hz
$f_p\langle \theta_I = 90^o \rangle$	peak noise frequency for core alone (single jet) at $\theta_I = 90^o$
h	annulus height, ft
K	constant defined by Eq. (2)
L_C	length of core nozzle extension beyond fan nozzle exit plane, ft
L_F	length of fan nozzle extension beyond core nozzle exit plane, ft
OASPL	overall sound pressure level, dB
PWL	sound power level, dB
PWL_T	total sound power level, dB
R	distance from noise source (in experiments, the fan nozzle exit) to observer or microphone, ft
SPL	sound pressure level, dB
SPL_p	peak intensity or sound pressure level, dB
T_o	environment temperature, ^oF
t	core nozzle lip thickness, ft
V_C	core jet velocity at nozzle exit plane (measured or calculated) based on one-dimensional isentropic theory, ft/sec

V_E maximum velocity of decaying flow at extended nozzle exit plane, ft/sec

V_F fan jet velocity, ft/sec

V_o third (outer) nozzle jet velocity, ft/sec

VR fan to core velocity ratio, V_F/V_C

$\Gamma\langle VR,AR\rangle$ function relating coaxial nozzle noise level relative to that of the core, defined by Eq. (3)

θ_I angle from nozzle inlet, deg

θ_J angle from nozzle jet, $\theta_J = 180 - \theta_I$, deg

ρ_o density of environment, lb_m/ft^3

References

1. Williams, T. J., Ali, M. R. M., and Anderson, J. S., "Noise and Flow Characteristics of Coaxial Jets," Journal of Mechanical Engineering Science, Vol. 11, No. 2, Apr. 1969, pp. 133-142.

2. Bielak, G. W., "Coaxial Flow Jet Noise," D6E-10041-1, 1972, Boeing/ Aeritalia Co., Seattle, Wash.

3. Eldred, K., "Far Field Noise Generation by Coaxial Flow Jet Exhausts. Vol. I: Detailed Discussion," FAA-RD-71-101-Vol. 1, 1971, Wyle Laboratories, Inc., El Segundo, Calif.

4. Anon., "Standard Values of Atmospheric Absorption as a Function of Temperature and Humidity for Use in Evaluating Aircraft Flyover Noise," Aerospace Recommended Practice 866, Aug. 31, 1964, SAE.

5. Olsen, W. A., Miles, J. H., and Dorsch, R. G., "Noise Generated by Impingement of a Jet Upon a Large Flat Board," TN D-7075, 1972, NASA.

6. Olsen, W. A., Gutierrez, O. A., and Dorsch, R. G., "The Effect of Nozzle Inlet Shape, Lip Thickness, and Exit Shape and Size on Subsonic Jet Noise," AIAA Paper 73-187, Washington, D.C., 1973.

7. Lush, P. A., "Measurements of Subsonic Jet Noise and Comparison with Theory," Journal of Fluid Mechanics, Vol. 46, Pt. 3, Apr. 1971, pp. 477-500.

8. Karchmer, A., Dorsch, R., and Friedman, R., "Acoustic Tests of 15.2-Centimeters Diameter Potential Flow Nozzle," TM X-2980, 1974, NASA.

9. Goldstein, M. E., and Howes, W. L., "New Aspects of Subsonic Aerodynamic Noise Theory," TN D-7158, 1973, NASA.

10. Goldstein, M., and Rosenbaum, B., "Effect of Anisotropic Turbulence on Aerodynamic Noise," Journal of the Acoustical Society of America, Vol. 54, No. 3, Sept. 1973, pp. 630-645.

11. Anon., "Jet Noise Prediction," Aerospace Information Rept. 876, SAE, July 1965.

12. Staff, "Aircraft Engine Noise Reduction," NASA SP-311, 1972, pp. 32-33, 58-59, 186, 187, 190, 202, 204, 206, 211-213.

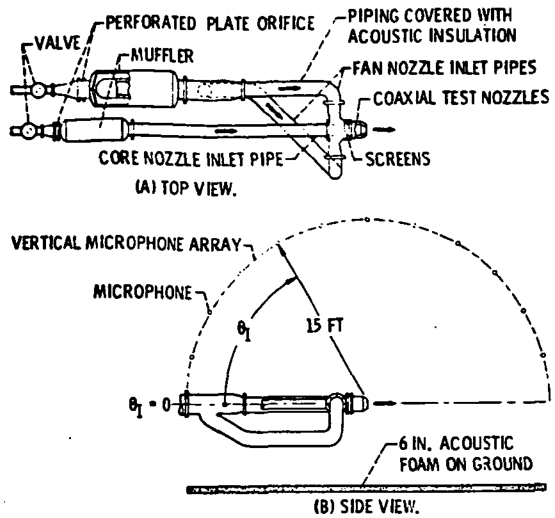

Figure 1. - Flow system for coaxial nozzle tests.

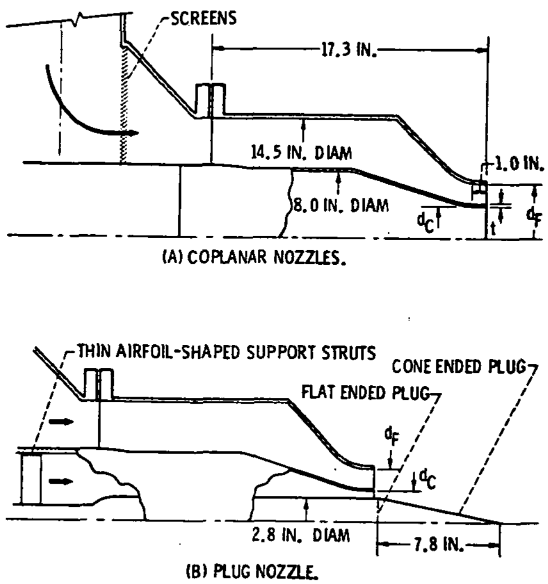

Figure 2. - Sketches of coaxial nozzles tested.

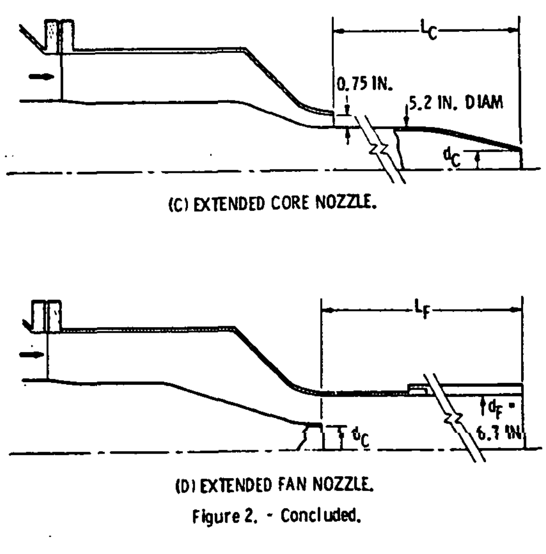

Figure 2. - Concluded.

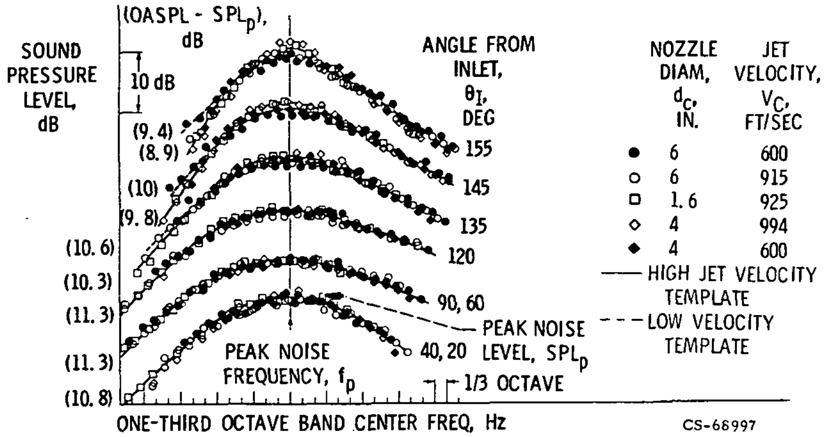

Figure 3. - Single stream (core) jet noise spectra shapes (templates). Ambient temperature subsonic circular jet; free field lossless data.

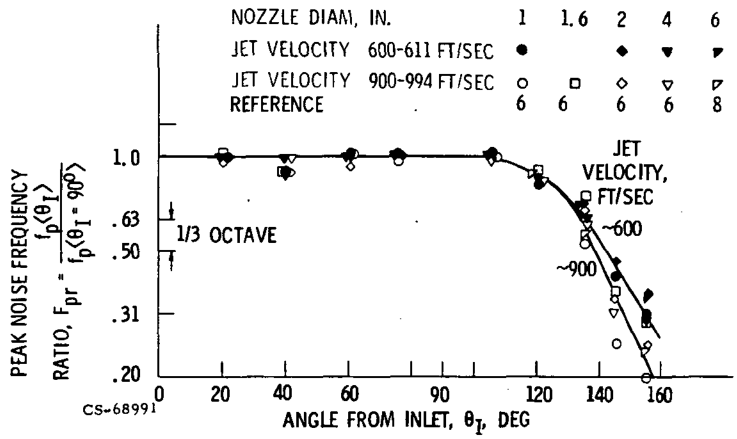

Figure 4. - Variation of the peak noise frequency with angle. Ambient temperature subsonic circular nozzles; free field lossless data.

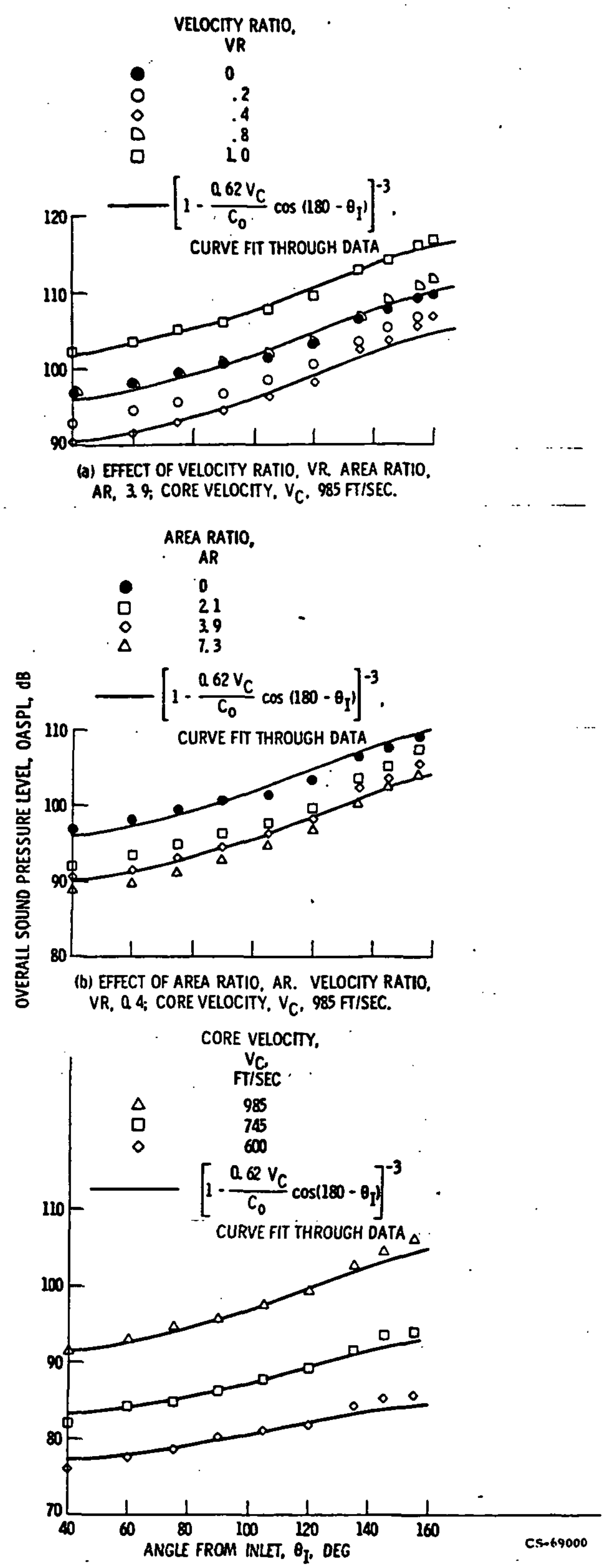

(c) EFFECT OF CORE VELOCITY, V_C. VELOCITY RATIO, VR, 0.6; AREA RATIO, AR, 3.9.

Figure 5. - Noise radiation pattern for coaxial nozzles at 15 feet. Core diameter, 3 in.; environmental temperature, 77° F; free field lossless data.

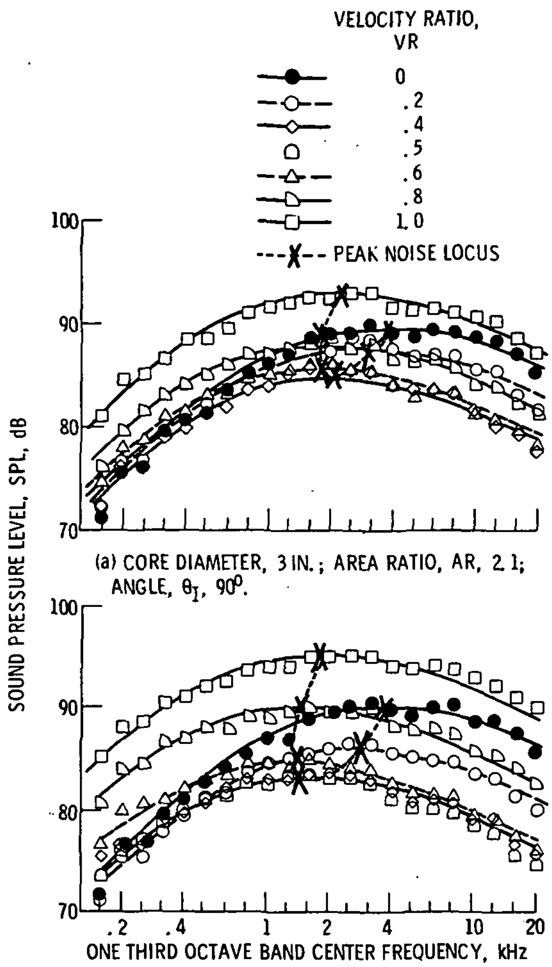

(a) CORE DIAMETER, 3 IN.; AREA RATIO, AR, 2.1; ANGLE, θ_I, 90°.

(b) CORE DIAMETER, 3 IN.; AREA RATIO, 3.9; ANGLE, 90°.

Figure 6. - Effect of velocity ratio on coaxial jet noise spectra. Coplanar circular nozzles; core jet velocity, V_C, 985 ft/sec; environmental temperature, 77° F; free field lossless data taken on a 15 foot radius. Curves through data are templates from figure 3.

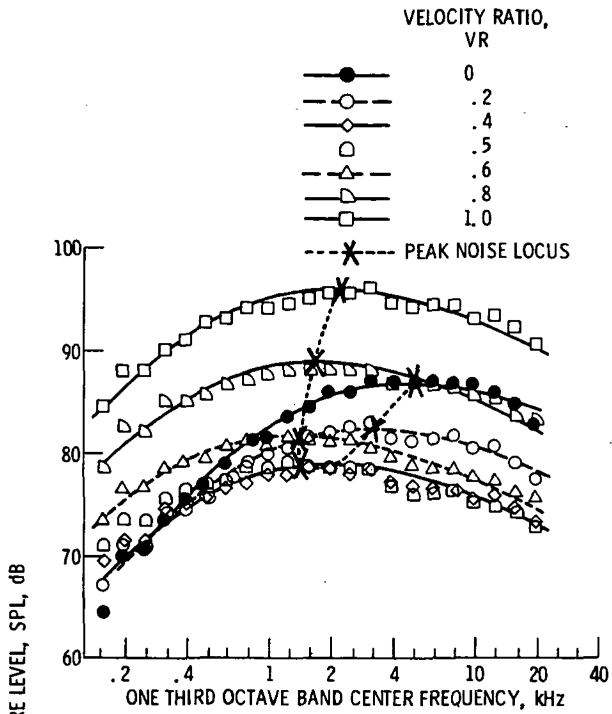

(c) CORE DIAMETER, 2.08 IN.; AREA RATIO, 9.3; ANGLE, 90°.

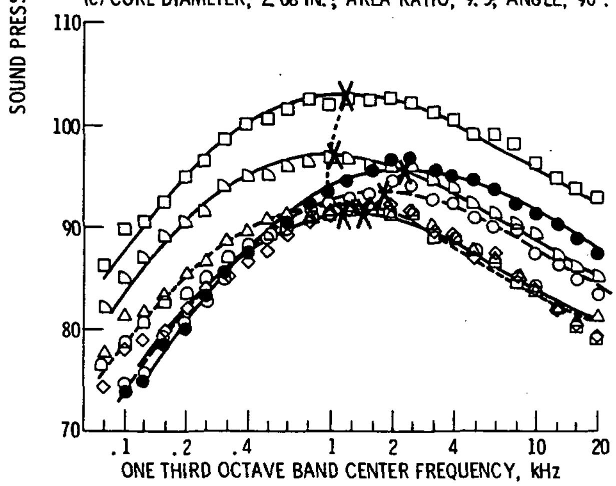

(d) CORE DIAMETER, 3 IN.; AREA RATIO, 3.9; ANGLE, 135°.

Figure 6. - Concluded.

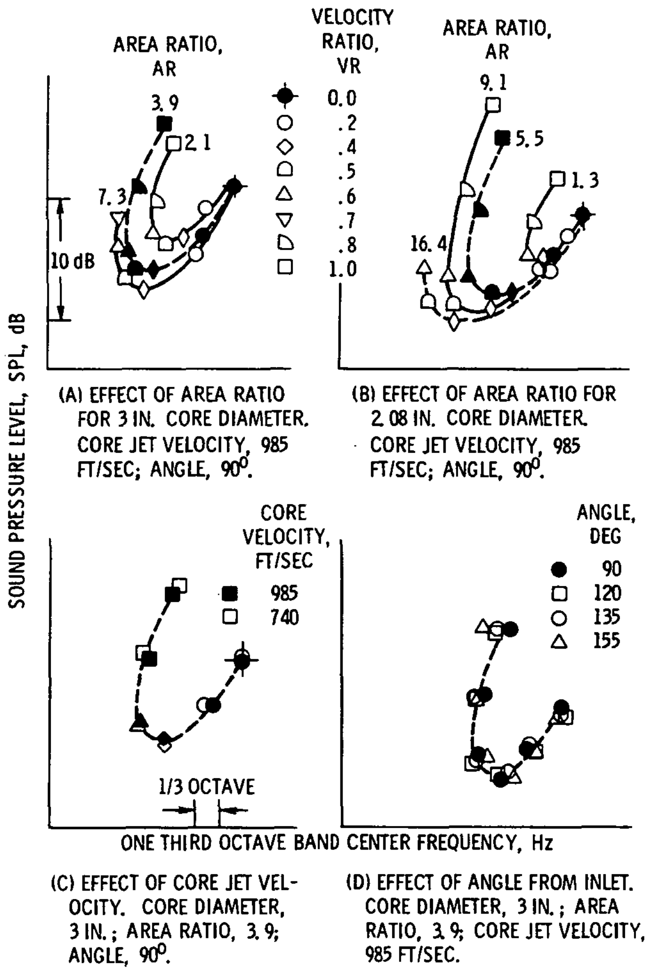

Figure 7. - Peak noise locus curve shapes for several coaxial nozzles. Circular coplanar nozzles; environmental temperature, 77° F; free field lossless data taken on a 15 foot radius.

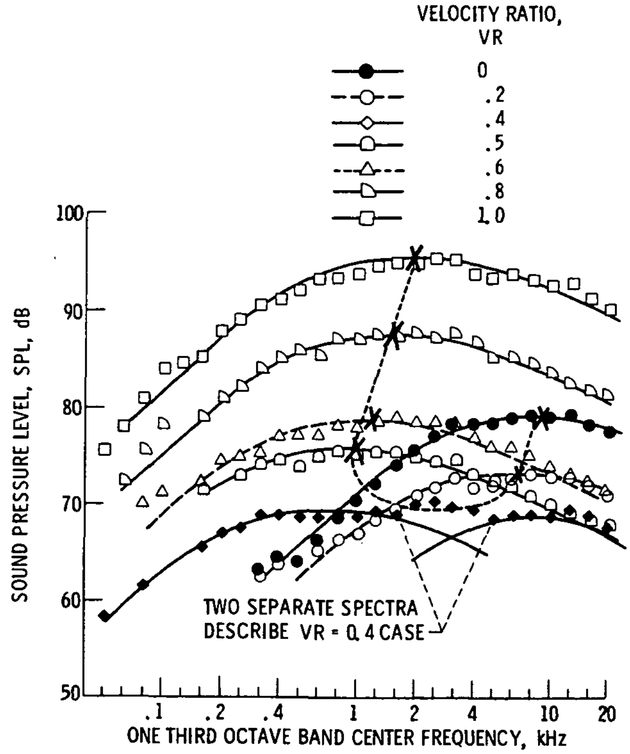

Figure 8. - Effect of velocity ratio on coaxial jet noise spectra at $\theta_I = 90^0$. Coplanar circular nozzles; area ratio, 43.5; core diameter, 1.0 inch; core jet velocity, 985 ft/sec; environmental temperature, 77^0 F; free field lossless data taken on a radius of 15 feet.

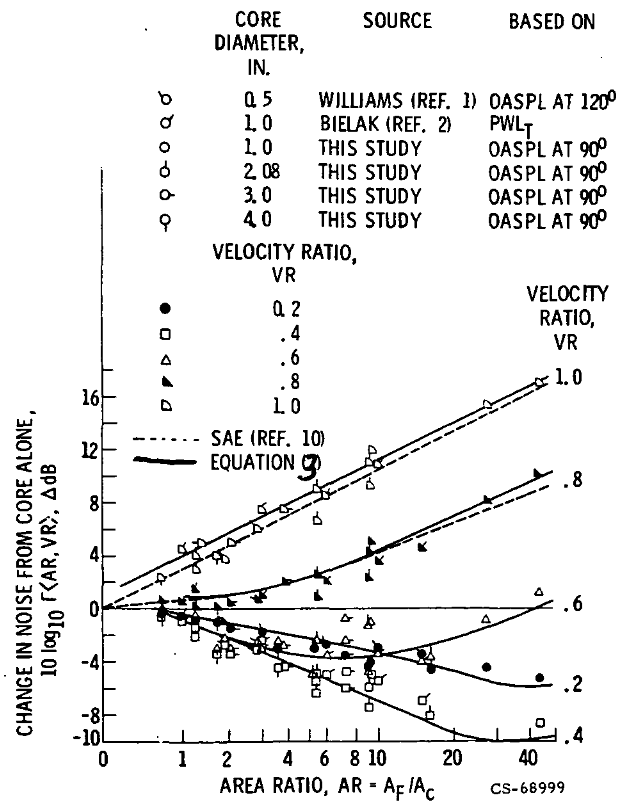

Figure 9. - Change in coaxial noise level, relative to the core alone noise level, with changes in area and velocity ratio.

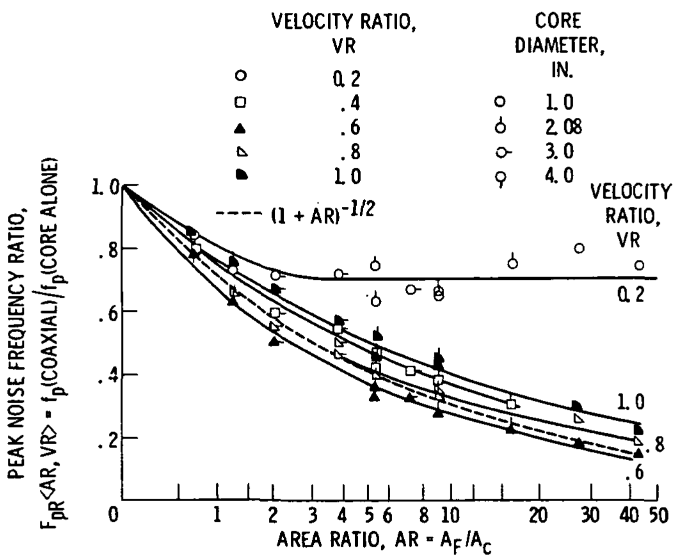

Figure 10. - Variation in peak noise frequency, relative to the core alone peak frequency.

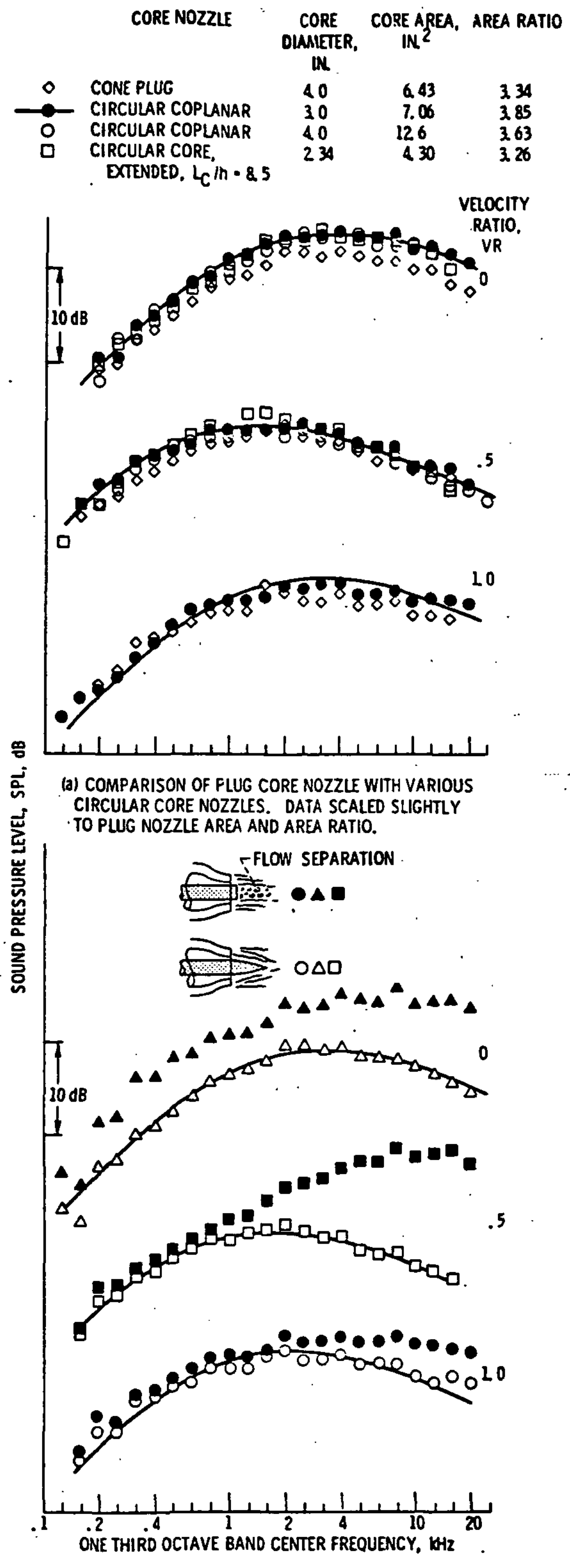

(a) COMPARISON OF PLUG CORE NOZZLE WITH VARIOUS CIRCULAR CORE NOZZLES. DATA SCALED SLIGHTLY TO PLUG NOZZLE AREA AND AREA RATIO.

(b) EFFECT OF FLOW SEPARATION OFF PLUG.

Figure 11. - Effect of a plug core nozzle on noise spectra at 90°. Plug diameter, 2.8 inch; core velocity, 985 ft/sec; environmental temperature, 77° F; free field lossless data taken on a 15 feet radius.

VELOCITY RATIO, VR = V_F/V_C	CORE LENGTH/ANNULUS HEIGHT L_C/h	
	8.5	56.0
1.0	□	■
.5	△	▲
0	○	●
V_E/V_F	1.0	0.5

CURVES DRAWN FROM PWL SPECTRAL SHAPE IN REF. 6

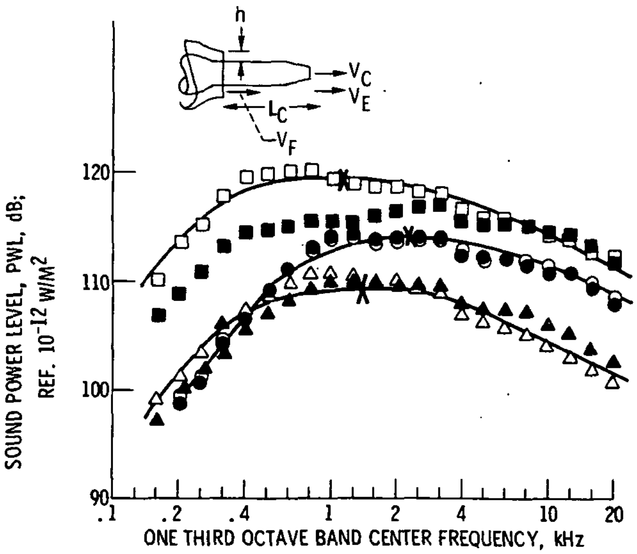

Figure 12. - Effect of a long core nozzle extension. Annulus height, h, 0.75 in.; core nozzle exit diameter, 2.34 in.; area ratio, 3.26, core jet velocity, 985 ft/sec. Environmental temperature, 77° F; free field lossless data.

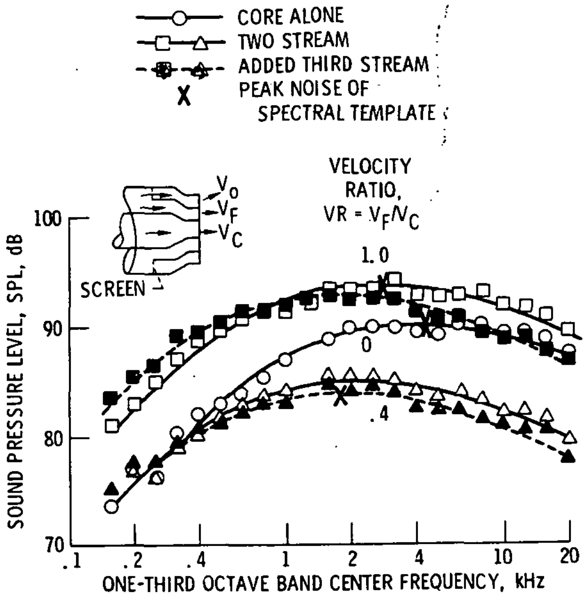

Figure 14. - Effect of a third nozzle exhaust stream. Core diameter, 3 inches; fan to core ratio, A_F/A_C = AR, 2.1; outer to fan area ratio, A_0/A_F, 0.78; core jet velocity, 985 ft/sec; nominal outer to fan velocity ratio, V_0/V_F, 0.75; environmental temperature, 77° F; free field lossless data on a 15-foot radius.

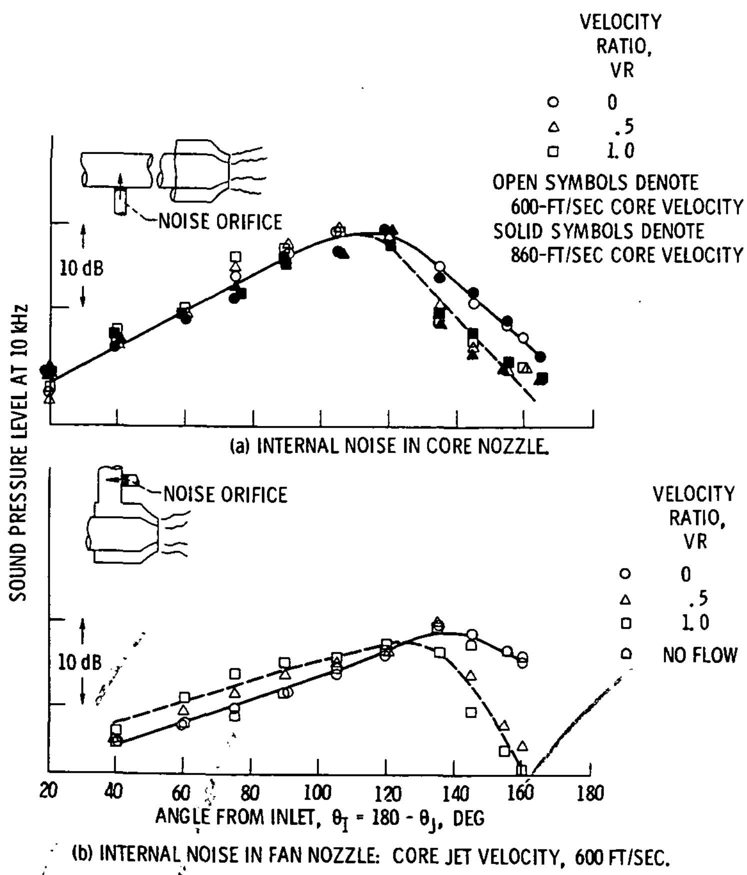

Figure 15. - Noise radiation pattern at 10 kHz of a dominant internal noise. Core diameter, 3 inches; area ratio, 2.1; noise orifice pressure ratio, 5.4.

FAN EXTENSION, L_F/d_F		EXIT VELOCITY, V_E/V_C			
		VR = 0	0.5	0.8	1.0
■	0	1.0	1.0	1.0	1.0
△	2	.72	.97	.99	.95
◇	4	.28	.92	.98	.98
○	6	.21	.89	.97	1.01

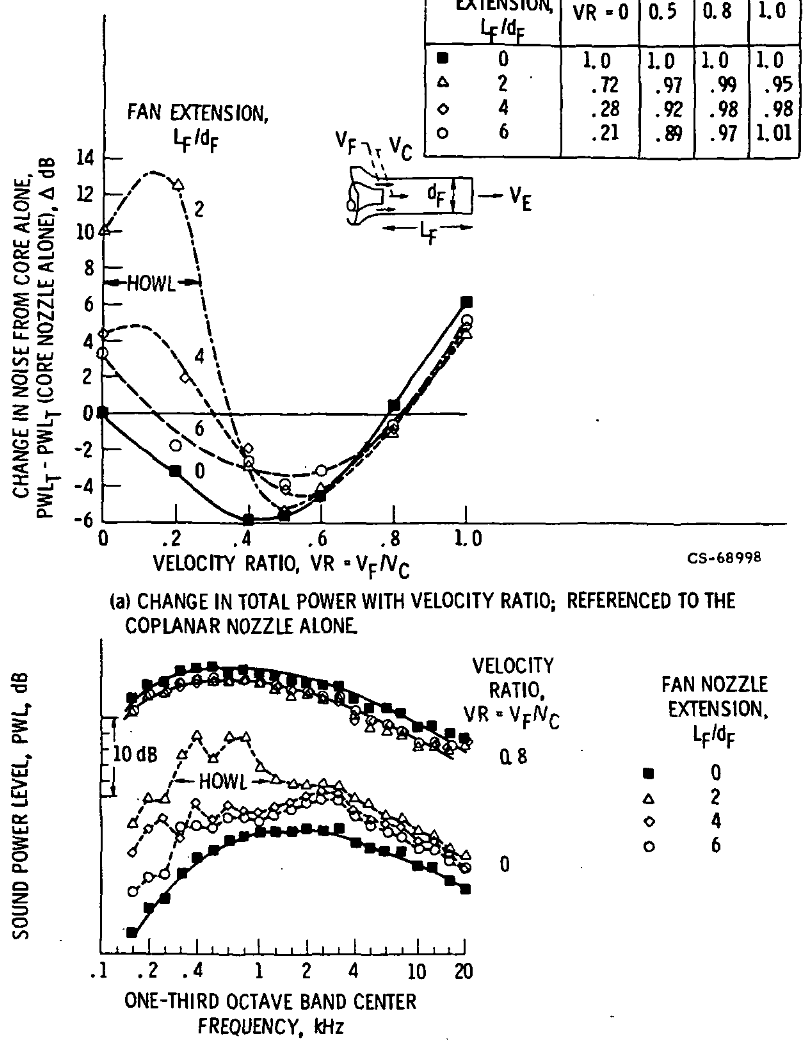

(a) CHANGE IN TOTAL POWER WITH VELOCITY RATIO; REFERENCED TO THE COPLANAR NOZZLE ALONE.

(b) POWER SPECTRA AT A HIGH AND LOW VELOCITY RATIO.

Figure 13. - Effect of fan nozzle extension pipe. Core diameter, 3 inches; area ratio, 3.9; core jet velocity, 740 ft/sec; environmental temperature, 77° F; free field lossless data.